T VIOLATION IN $K^+ \to \pi^0\mu^+\nu_\mu$ AT KEK

Jun Imazato

Institute of Particle and Nuclear Studies

High Energy Accelerator Research Organization

Tsukuba-shi, Ibaraki-ken, 305-0801 Japan

Representing the E246 Collaboration[1]

ABSTRACT

The transverse muon polarization in $K^+ \to \pi^0\mu^+\nu_\mu$ is a measure of T violation and a good probe of CP violation from physics beyond the Standard Model. The KEK E246 experiment is searching for the transverse polarization using a new technique with stopped kaons in conjunction with a Superconducting Toroidal Spectrometer. With such a high performance detector, a measurement with low backgrounds and small systematic errors can be realized. Data taking began in 1996 and analysis has now been completed for the data obtained until the end of 1997. There is no sign of T violation found within the experimental errors. The sources of systematic errors have been carefully studied with the conclusion that the total systematic error is far below the current statistical error.

1 Transverse Muon Polarization in $K^+ \to \pi^0 \mu^+ \nu_\mu$

$K^+ \to \pi^0 \mu^+ \nu_\mu$ decay ($K_{\mu 3}$) provides a unique possiblity to test the violation of time reversal invariance (T violation) in kaon decay through the transverse muon polarization (P_T), which is the polarization component normal to the decay plane. P_T is expressed in terms of a triple vector correlation of the muon spin $\vec{\sigma}_\mu$ and the momentum vectors $\vec{p}_\pi, \vec{p}_\mu$, of the pion and muon as

$$P_T = \frac{\vec{\sigma}_\mu \cdot (\vec{p}_\pi \times \vec{p}_\mu)}{|\vec{p}_\pi \times \vec{p}_\mu|}, \qquad (1)$$

which is T-odd; thus nonvanishing P_T would be a clear sign of T violation.[2] The spurious effect from final state interactions is known to be as small as 10^{-6} in this charged kaon decay case[3] because there is only one charged particle in the final state. Under the assumption of CPT invariance, the search for T violation can address the origin of CP violation. Since the contribution from the Standard Model is only from higher orders which are negligibly small $\sim O(10^{-6})$, P_T can be a sensitive probe of additional Non-Standard Model sources of CP violation. Various theoretical models, such as the multi-Higgs model and the leptoquark model, can produce a sizable effect in P_T at the level of 10^{-3}, which is experimentally detectable, without conflicting with the present constraints from other experimental channels.[4,5] More recently, a class of supersymmetric models,[6,7] such as the R-parity violation model, have also been examined and shown to have a potentially large contribution to P_T. From these theoretical points of view, a P_T search with a sensitivity of 10^{-3} is of great interest.

The $K_{\mu 3}$ process is described in the V-A scheme in terms of a decay amplitude with two form factors $f^+(q^2)$ and $f^-(q^2)$ as

$$M \propto \frac{G_F}{2} \sin\theta_C [f^+(q^2)(\tilde{p}_K^\lambda + \tilde{p}_\pi^\lambda) + f^-(q^2)(\tilde{p}_K^\lambda - \tilde{p}_\pi^\lambda)] \cdot [\bar{u}_\mu \gamma_\lambda (1 - \gamma_5) u_\nu], \qquad (2)$$

with four momenta $\tilde{p}_K$ and $\tilde{p}_\pi$ of the kaon and pion, respectively. A complex phase between $f^+(q^2)$ and $f^-(q^2)$ induces T violation. Using the definition, $\xi \equiv f^-/f^+$, P_T can be written as

$$P_T = Im\xi \cdot \frac{m_\mu}{m_K} \cdot \frac{|\vec{p}_\mu|}{E_\mu + |\vec{p}_\mu| \vec{n}_\mu \cdot \vec{n}_\nu - m_\mu^2 / m_K}. \qquad (3)$$

Thus, $Im\xi$ is the measure of T violation in $K_{\mu 3}$ decay independent of decay kinematics. In the three-Higgs doublet model with natural flavor conservation[4,5,8] for example, the decay can proceed via charged Higgs exchange, contributing mainly to f^-, and a sizable effect on P_T appears due to the interference with the normal W exchange term. $Im\xi$ can be expressed as

$$Im\xi = Im(\alpha_1 \beta_1^*) \cdot \frac{v_2^2}{v_3^2} \cdot \frac{m_{K^+}^2}{m_{H^+}^2}, \qquad (4)$$

where α_i and β_i are the coupling coefficients of the interaction in the mass eigenstate of the Higgs boson with down-type quarks and up-type quarks, respectively, and v_2/v_3 is the ratio of the Higgs field vacuum expectation values. P_T thus constrains the two parameters, $Im(\alpha_1 \beta_1^*)$ and v_2/v_3. The former parameter is solely constrained by non-leptonic processes, such as the neutron electric dipole moment[9] and $b \to s\gamma$.[10] However, $Im\xi$ can constrain it more stringently for the large v_2/v_3 region, which may be relevant in a scenario[4] where the v_i's are proportional to the fermion masses to which they couple, i.e., with $v_2/v_3 \propto m_t/m_\tau \sim 100$. The semileptonic $B \to \tau\nu_\tau X$ decay can provide similar constraints to the parameters as does $Im\xi$ (Ref. 10).

A search for T violation in $K_{\mu 3}$ decay has been attempted before in both K^+ and K_L^0 decays. The most recent data for K^+ come from a BNL-AGS experiment more than 15 years ago,[11] giving a limit of P_T(lab)$= (-0.31 \pm 0.53) \times 10^{-2}$ and $Im\xi = -0.016 \pm 0.025$. This K^+ experiment used an in-flight decay method detecting a photon from the pion decaying in the direction of the beam. A similar K_L^0 decay experiment, also done at BNL-AGS, gave a similar limit, P_T(lab)$= (0.21 \pm 0.48) \times 10^{-2}$ and $Im\xi = 0.009 \pm 0.030$ (Ref. 12). However, in the case of the K_L^0 decay, one suffers from large final state interaction effects of nearly 10^{-2}. Therefore, K^+ decay is uniquely suited for a high-precision experiment at the present time.

2 KEK E246 Experiment

2.1 Stopped Beam Method and Setup

In a P_T search experiment, it is necessary to detect a tiny P_T component in the presence of the large T conserving in-plane polarization components, P_L and P_N, which are parallel and perpendicular to the muon momentum vector, respectively. In order to overcome this difficulty, the KEK E246 experiment adopted a stopped K^+ method in conjunction with a Superconducting Toroidal Spectrometer. Using these two basic strategies we are aiming not only for an improvement of the statistical accuracy compared to the previous limit, but also for a measurement with a substantial reduction of the many systematic errors to the 10^{-3} level for ΔP_T. The advantages of using a

stopped kaon beam are manifold, but the most important is the near total coverage of $K_{\mu3}$ decay kinematics by the detector. This enables us to carry out a measurement of the decay phase-space region with an opposite contribution to P_T. Namely, we can perform a double-ratio measurement with enhanced sensitivity to P_T, while suppressing systematic errors drastically. Moreover, the decay phase-space includes a region with vanishing P_T, providing us with the opportunity for a null-effect check. Other merits of this method, compared with in-flight decay experiments, are the small influence of a finite beam emittance, low backgrounds, smaller counting rates in each detector element, and a relatively short length of the detector.

Figure 1 shows the cross section and end view of the setup. The Superconducting Toroidal Spectrometer has a large acceptance as well as a high momentum resolution for the analysis of charged particles from the stopped kaon decay in the central region of the magnet. This allows a high statistics measurement with efficient background rejection. Furthermore, the magnet has precise 30-degree rotational symmetry, which is essential in an asymmetry experiment in order to reduce a number of systematic effects. A positive kaon beam with a momentum of 660 MeV/c was slowed down through an Al+BeO degrader and stopped in an active target made of a bundle of scintillating fibers at the center of the magnet. The $K_{\mu3}$ decay was identified by detecting both the π^0 and the μ^+. The pion was detected as two-γ or one-γ by a calorimeter which comprises 768 CsI(Tl) crystals surrounding the target. The muon was accepted by one of the 12 magnet gaps, momentum-analyzed in a 0.9 T field, and then stopped in a muon stopper located at the exit of the magnet gap, where the polarization measurement takes place. At the stopper, there was a field applied to hold the transverse component of the polarization, while precessing the in-plane components.

2.2 Double-Ratio Experiment

The P_T of the stopped muon manifests itself as either a clockwise (cw) or counterclockwise (ccw) asymmetry in the polarimeter, depending on the emission angle of the pion relative to the beam axis. It is measured by means of the decay positron cw/ccw asymmetry as

$$\frac{\sum_{i=1}^{12} N_i(cw)}{\sum_{i=1}^{12} N_i(ccw)} \cong 1 + 2\alpha\langle\cos\theta_T\rangle P_T. \tag{5}$$

Here, α is the analyzing power including four factors: (i) the intrinsic asymmetry of 1/3, (ii) the attenuation due to finite counter solid angle, (iii) the attenuation factor of P_T due to precession in the imperfect parallel field, and (iv) the effects of positron
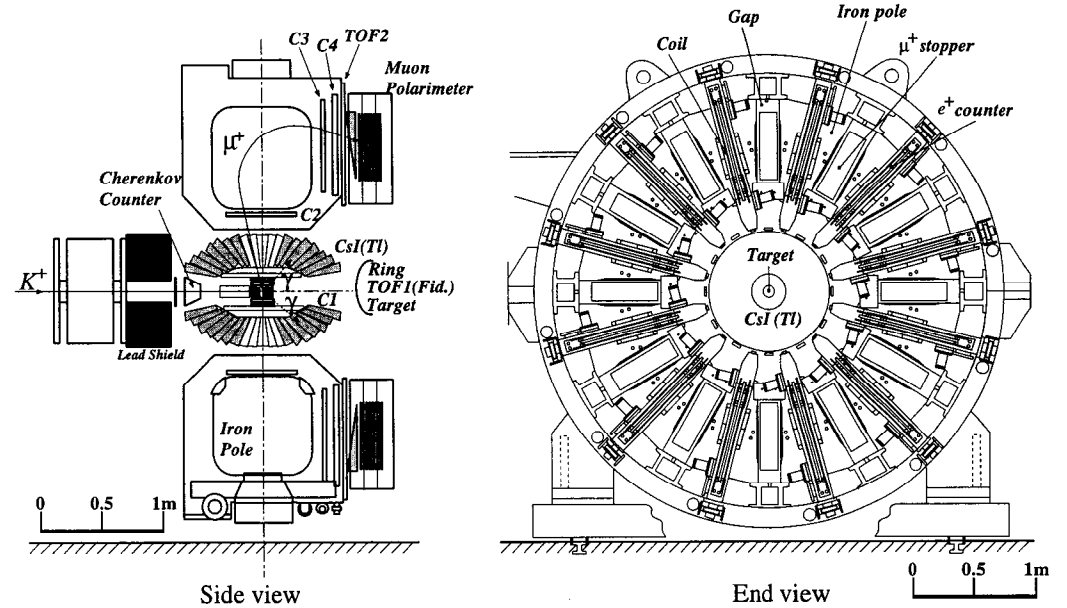

Fig. 1. Cross-section view and end view of the E246 detector.

scattering and absorption. The factor $\langle \cos \theta_T \rangle$ is the kinematic attenuation of P_T due to the distribution of decay planes in the finite acceptance of the detector. The magnetic field at the stopper was carefully trimmed to assure a symmetric distribution of the field across the magnet median plane, so that there should be no effect from P_L and P_N in total. By summing over the 12 gaps, several systematics, such as the effect of an asymmetric kaon stopping distribution in the target and unequal detection efficiency of positron counting, can be cancelled. In the actual measurement, we take the double ratio of Eq. (5) for the cases of π^0 going into the forward and the backward directions

$$\frac{[\sum_{i=1}^{12} N_i(cw)/\sum_{i=1}^{12} N_i(ccw)]_{fwd}}{[\sum_{i=1}^{12} N_i(cw)/\sum_{i=1}^{12} N_i(ccw)]_{bwd}} \cong 1 + 4\alpha\langle \cos \theta_T \rangle P_T, \quad (6)$$

which provides further cancellation of systematic errors, and is only possible in a stopped beam experiment. The sensitivity to $Im\xi$ for a given P_T is large at the high muon energy boundary on the Dalitz plane, but the decay intensity is large for the high pion energy region with the result that the figure-of-merit ($\sqrt{N}P_T/Im\xi$) distribution is concentrated in the central part of the Dalitz plane. The acceptance of the detector can cover this high figure-of-merit region by selecting the appropriate spectrometer magnetic field.

3 Detector Performance and Analysis

The main part of the E246 detector comprises μ^+ tracking systems, a π^0 detector, and muon polarimeters. It was designed to detect all the decay particles with high resolution and large acceptance. It was also designed to reduce the influence of accidental background arising from pions in the beam which are several times more numerous than the kaons.

3.1 μ^+ Tracking and Identification

The charged particles from the kaon decay are tracked by four sets of chambers C1, C2, C3, and C4, a scintillating fiber target, and a ring counter system surrounding the target. C1 is a cylindrical drift chamber with a helical cathode strip readout of the z (beam axis) coordinate together with anode signals for azimuthal information. The other chambers, located at the entrance and exit of the magnet gaps, are planar MWPC's with cathode readout for both x and y directions. The ring system[13] consists of 32 ring scintillator counters with a 118 mm inner diameter, 5 mm thickness, and 6 mm width, covering

Table 1. Main parameters of the target and ring systems.

Target		Rings	
Fiber size	5 mm × 5 mm × 2 m	Size of a ring	$5^T \times 6^W \times 119$ mm^{ID}
Number of fibers	256	Number of rings	32
Diameter	106 mm	Total length	20 cm
Fiducial length	20 cm	Readout	single turn WLS fiber
Information	x and y coordinate	Information	z coordinate

the 20 cm fiducial region of the target. This provides us with additional z-coordinate information under high rate conditions. Readout is by means of a wavelength-shifter fiber glued into a groove cut in each ring. A high light yield of 46 photoelectrons (pe) for a minimum ionizing particle was achieved. The active stopping target, consisting of 256 5×5 mm^2 scintillating fibers with direct individual PMT readout, serves both as one of the tracking elements as well as a means of decay vertex determination. The kaon stopping is identified as a signal with large energy deposit, while decay muons leave dE of minimum ionization. Figure 2 illustrates the target and ring assembly. The main parameters of the tracking system are summarized in Table 1.

Figure 3 shows the momentum spectrum of K-decay charged particles under a realistic trigger condition requiring a photon detection in the CsI(Tl) detector and a decay positron detection in the polarimeter. The resolution is dominated by multiple scattering in air and in the chambers, but is sufficient for the purpose of the $K_{\mu 3}$ selection. The predominant background peak from $K_{\pi 2}$ pions stopping in the muon stopper can be readily rejected by setting a momentum threshold at 190 MeV/c. The $K_{\mu 3}$ events are distributed in the bump below 190 MeV/c together with K_{e3} positrons, which can be rejected by using TOF information between a counter at the exit of the magnet gap and the target fiducial counter. Otherwise, these K_{e3} positrons, when scattered by the copper degrader and the stopper, contribute to the background in the muon-decay positron time spectrum as a prompt timing peak. The performance of the TOF separation is shown in Fig. 4.
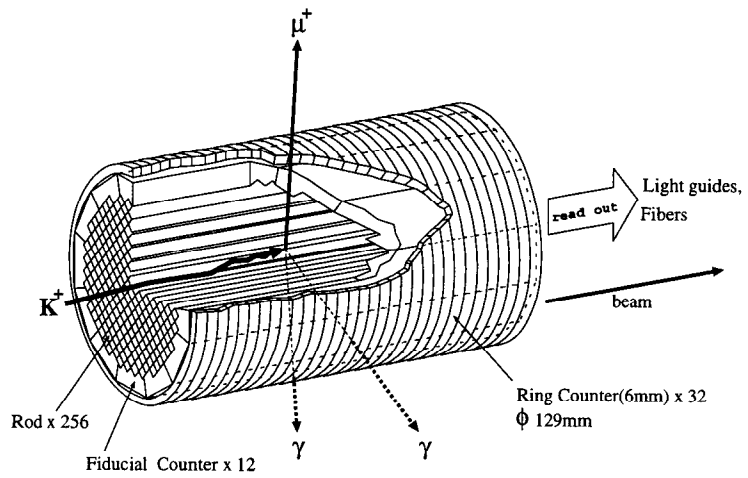
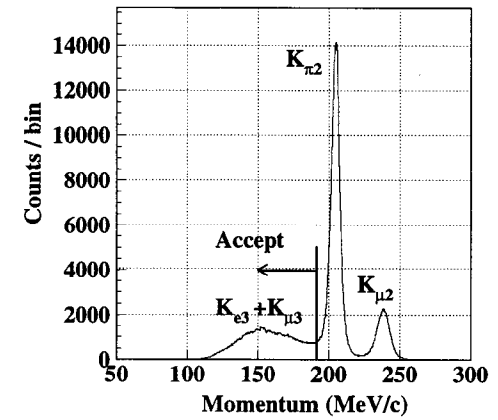Fig. 2. Schematic view of the active target and ring counter system.

Fig. 3. Momentum spectrum of charged particles under the trigger condition of photon detection in the CsI(Tl) and positron detection in the positron counters. The $K_{\mu 2}$ peak is due to an accidental photon in the CsI(Tl).
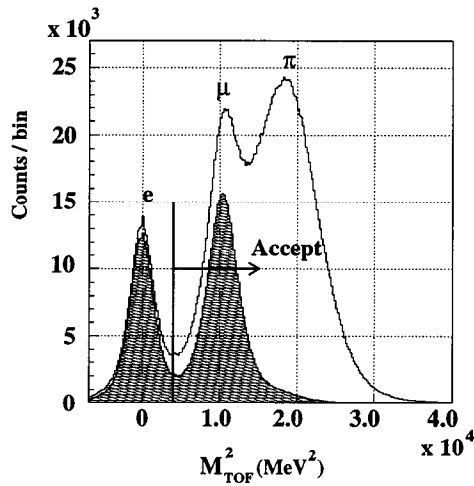
Fig. 4. TOF mass spectrum of charged particles before momentum selection (solid line) and after momentum selection (shaded spectrum).

3.2   CsI(Tl) π^0 Detector

The π^0 detector[14,15] is a barrel array of 768 CsI(Tl) crystals surrounding the target with a solid angle of about 3/4 of 4π. The barrel is segmented with $\Delta\theta = \Delta\phi = 7.5°$, both for polar and azimuthal directions, except for one layer nearest to the beam axis where $\Delta\phi = 15°$. There are 12 rectangular holes for charged particles to enter the magnet gaps and two holes for the beam entrance and exit (Fig. 5). The main parameters of each crystal module and the whole detector are summarized in Table 2. Because of space problems in the central region of the magnet and the existence of a fringing field, PIN photodiode readout was employed. Very high performance of these CsI modules was achieved with an average light yield as high as 11,000 pe/MeV with an equivalent noise level (EVL) of 65 keV.[15] This low-noise level allowed us to lower the photon detection threshold to 5 MeV. The signal from each diode is read by a peak-sensing ADC after pulse shaping and at the same time by a pulse shape analyzer by means of a transient digitizer.[16] A timing resolution of 13 ns (FWHM) was obtained in the relevant energy region by means of a constant fraction discriminator trigger.[17] This excellent timing performance was very powerful in identifying photon clusters and rejecting backgrounds. In spite of the large lateral shower leakage, a relatively narrow invariant mass spectrum is observed. Figure 6 shows the spectra for π^0 in the forward or backward directions in which photons are likely to hit a nonhole region, and in the normal direction in which photons hit mostly muon holes, respectively.

The clean π^0 events consisted of two photons in the CsI. In order to recover some of the π^0 acceptance lost due to the holes in the CsI array, we also accepted events with only one–photon cluster, satisfying a high-energy threshold (70 MeV), for which most of the π^0 kinematic information was preserved.

3.3   Muon Polarimeter

The structure of the muon polarimeter is shown schematically in Fig. 7. Muons are bent in the magnet gap, slowed down through a wedge-shaped copper degrader, and stopped in a muon stopper made of plates of pure Al. In order to minimize the effect of scattering and absorption for the decay positrons, the plates are spaced to give an effective density of 0.4 of bulk Al. The material has been studied in a muon spin rotation measurement and it was confirmed that there is no significant depolarization during the stopping process nor any relaxation due to solid state effects. At the stopper, a magnetic field was applied using pure-iron shim plates to conduct a fraction of the
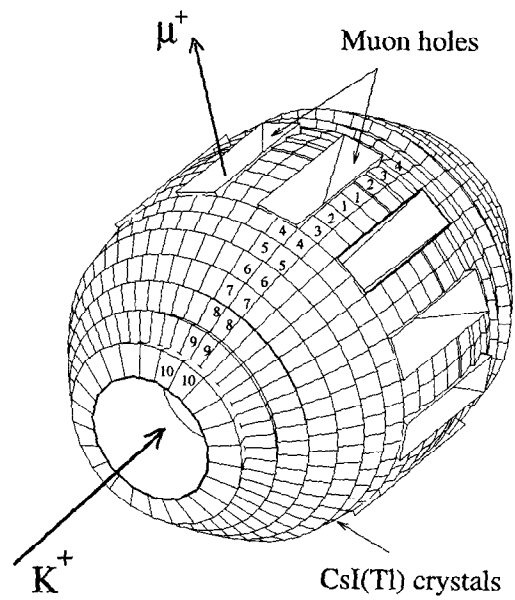
Fig. 5. CsI(Tl) π^0 detector. There are 12 rectangular holes for the charged particles to enter the magnet gaps.
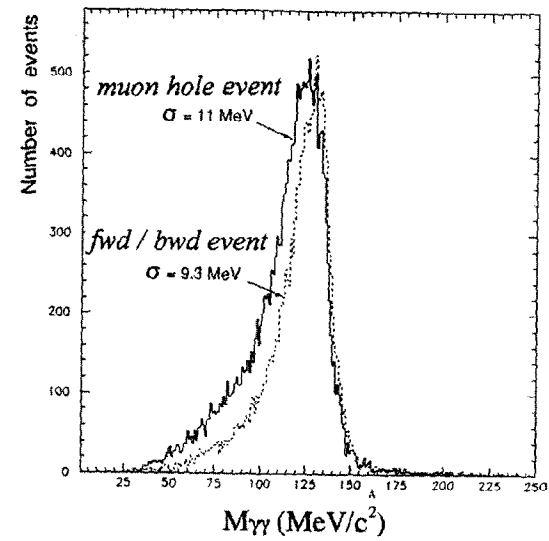

Fig. 6. Invariant mass spectrum for two-γ; the dotted line is for the events with a pion in the forward or backward directions, and the solid line is for the events with a pion in the direction perpendicular to the beam.

Fig. 7. Schematic view of the polarimeter of one gap.

Table 2. Main parameters of the CsI(Tl) π^0 detector.

Structure		Performance	
Number of crystals	768	Readout	PIN photodiode
Segmentation	$\Delta\theta = \Delta\phi = 7.5°$	Light yield	$11000\,pe/\mathrm{MeV}$
Length of crystal	25 cm	ENL	65 keV
Typical size	$3 \times 3 - 6 \times 6$ cm	Time resolution	6.5 ns (σ)
Inner radius	20 cm	Energy resolution	3.0% at 200 MeV
Outer radius	50 cm	Position resolution	1.0 cm
Total weight	1.7 ton	Energy threshold	5 MeV

superconducting magnet fringing field. The shim plates were designed so as to make a strong field on the stopper and also to accomplish symmetric distribution of the field relative to the magnet median plane. Thus, the average field direction is parallel to the average direction of P_T, and the spurious effects arising from P_L and P_N should be cancelled in total, although the field flux is curving between the two shim plates. Field mapping was performed with a specially designed high-precision device with a three-dimensional Hall probe,[18] and the excellent symmetry of the field was confirmed.

Decay positrons were measured by counter systems located between each pair of adjacent muon stoppers. Each counter system consists of three layers of plastic scintillators, the middle one being segmented into three parts. The alignment of the polarimeter elements was done with particular care. The rear and outer sides of the stoppers were surrounded by veto counters to suppress background events from muons stopping outside the stoppers and from accidental room background. A large fraction of the background associated with the beam could be suppressed by a veto counter system surrounding the central region of the polarimeter. Figure 8 shows the time spectrum of positrons in good events recorded by a multistop TDC before and after the background suppression. A very low level of constant background of 13% for the signal region up to 8 μsec was achieved. There is a small structure seen at the beginning of the decay period due to the spin precession of the in-plane component. The $K_{\mu3}$ events were extracted by subtracting the constant background from the signal region of the time spectrum.
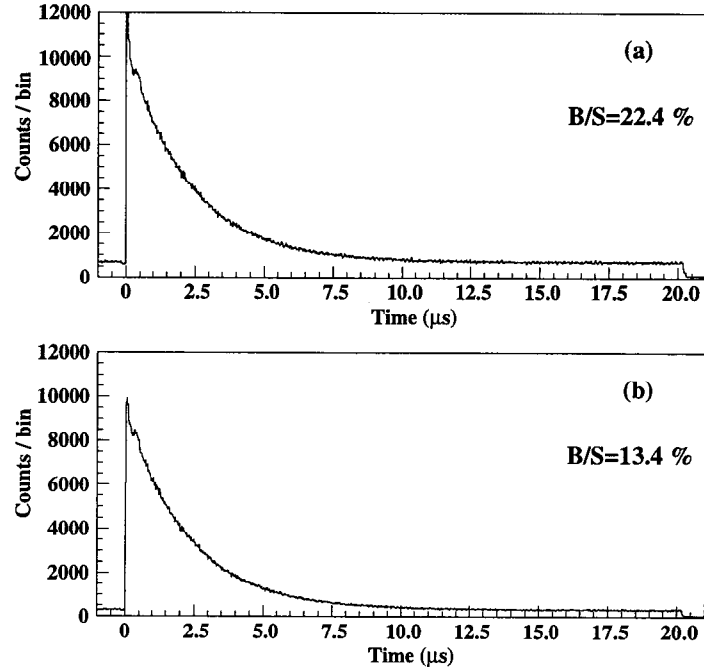
Fig. 8. Positron time spectra: (a) before applying veto counters, and (b) after applying veto counters. B/S was calculated for the signal region from 0 to 8μsec.

Table 3. Main parameters of the muon polarimeter.

Stopper		Counters	
Material	pure Al	e^+ detection	three fold of plastics
Size of a plate	$0.6^T \times 55^H \times 16^W \text{cm}^3$	Size	$84^H \times 30^W \text{cm}^2$
Number of plates	8	Segmentation	three middle layers
Spacing	0.8 cm	Solid angle $/4\pi$	0.07
Effective ρ	0.43 ρ_{Al}	Muon gate	20 μsec

3.4 Analysis

Good $K_{\mu3}$ events were selected by setting cuts on the (a) momentum spectrum, (b) invariant mass spectrum and photon total energy (in the case of two-γ), (c) single photon energy (in the case of one-γ), (d) mass spectrum from TOF, and (e) kaon decay time spectrum. A kinematic cut on the opening angle between the muon and the pion was very useful for rejecting any $K_{\pi2}$ pions remaining from the momentum cut and their decay-in-flight muons. Finally, the missing-mass cut was tuned to reject events from kaon decay-in-flight. Events were analyzed separately for the two-γ and one-γ cases. The regions of analysis, π^0–forward and π^0–backward, were determined to be $| \cos \theta_{\pi^0} |$, $| \cos \theta_\gamma | > 0.34$ both for two-γ and one-γ events by maximizing the figure-of-merit function $\langle \cos \theta_T \times P_T / Im\xi \rangle \times \sqrt{N}$; here, θ_{π^0} and θ_γ are the polar angles of the π^0 or one-γ, respectively. The asymmetry, A_T, was extracted from the ratio of cw and ccw positron counting, and P_T was calculated as

$$P_T = \frac{A_T}{\alpha \langle \cos \theta_T \rangle}. \tag{7}$$

The analyzing power α was deduced to be 0.198 by measuring the asymmetry from the in-plane polarization P_N by selecting events with the π^0 going into the Cs(Tl) barrel perpendicular to the beam axis. The kinematic attenuation factor $\langle \cos \theta_T \rangle$ was calculated in a Monte Carlo simulation taking into account the beam accidental background, which could be estimated from $K_{\mu2}$ events in coincidence with accidental photons. P_T was then converted to $Im\xi$ using an average sensitivity factor $\langle P_T / Im\xi \rangle$ also estimated by a Monte Carlo calculation,

$$Im\xi = \frac{P_T}{\langle P_T / Im\xi \rangle}. \tag{8}$$

4 Current Status of E246

4.1 Statistical Limit

After the detector construction from 1992 to 1995, we started data acquisition in early 1996. Using the low momentum K^+ beam from the K5 beam channel at the KEK proton synchrotron with intensity of 1.1×10^5/sec, we obtained a $K_{\mu 3}$ event rate of 1.0 /sec. By the summer of 1998, we had accumulated a total of 3.6 million events in the π^0–forward and π^0–backward regions. We are performing two independent analyses in the group. This should make the result more reliable because a consistency test can be done, and it also gives us a means of estimating the systematic errors associated with the analysis. The major differences in the two analyses lie in the charged particle tracking algorithm and in the photon clustering algorithm in the CsI(Tl) array. The near equivalence of the two analyses was checked by comparing good final events in both analyses and their correlations. However, some fraction of the good events belong only to one analysis, and the difference of the central values is attributed to the statistical fluctuations of this part. Both analyses have finished processing all the 1996 and 1997 data.[19–21] Both preliminary results are consistent with null-T violation within the statistical error

$$P_T = (-2.55 \pm 5.68) \times 10^{-3}, \; Im\xi = (-0.77 \pm 1.86) \times 10^{-2} \qquad (9)$$

for one analysis, and

$$P_T = (-0.25 \pm 5.72) \times 10^{-3}, \; Im\xi = (-0.01 \pm 1.80) \times 10^{-2} \qquad (10)$$

for the other. We are currently engaged in a discussion on how to best combine these two results. When the 1998 data has been analyzed, a statistical limit of $\Delta Im\xi = 0.011$ is expected.

4.2 Backgrounds

Although the main part of the $K_{\pi 2}$ background was rejected in the momentum spectrum as well as by an opening-angle cut, the decay-in-flight of pions into muon remains as an admixed background estimated to be a few percent of the good events. However, the average contribution to P_T for these events should be zero, and moreover, the forward/backward cancellation is expected to work, with no significant influence on the result. The contamination of other backgrounds, $K^+ \to \pi^+\pi^0\pi^0$ and $K^+ \to \pi^0 e^+\nu$,

was suppressed below 0.5% and 0.1%, respectively. These backgrounds should not produce any spurious asymmetry. The contamination of kaon decay-in-flight events was also suppressed below the 3–4% level by a cut on the missing mass and it was checked that there was no bias induced by its admixture. The amount of accidental background in the CsI(Tl) detector which is due to scattered pions in the beam was estimated to be 7–9% in both analyses, and its effect was taken into account as a degradation of the kinematic attenuation factor $\langle \cos\theta_T \rangle$ arising from the uncertainty in the decay plane determination.

4.3 Systematic Errors

The systematic errors were evaluated using real experimental data as well as Monte Carlo simulation. The most serious source is the asymmetry of the muon spin rotation field distribution. However, this effect could be estimated to be $\Delta P_T \leq 6 \times 10^{-4}$ from the measured tilt of the field distribution in each gap and from the uncertainty of the angular determination in the field mapping. The effects of a misalignment of the detector elements could be tested by examining the distributions of the decay plane orientation relative to the polarimeter coordinate frame. The average values of the plane tilt around the radial axis x and the beam axis z induce mixing of P_L and P_N, respectively, resulting in a fake effect. However, these effects were shown to be $\Delta P_T \approx 3 - 4 \times 10^{-4}$ each. The effective cancellation factor in the forward/backward ratio was evaluated from an artificial asymmetry distribution introduced by setting asymmetric cuts on the real data and then calculating the cancellation. The relatively large asymmetry of the kaon stopping distribution in the target due to the beam momentum dispersion was shown to have no first order influence on the result thanks to the cancellation mechanism when summing over the 12 gaps. The total systematic error was, thus, estimated to be $\Delta P_T = 1.0 \times 10^{-3}$, which is more than five times smaller than the current statistical error. The overall systematics could be further checked in (1) the null asymmetry with the pion integrated over all directions, (2) the gap dependence of the asymmetry, and (3) the polar angle dependence of the asymmetry; no systematic bias nor any strange magnet gap dependence was found.

5 Summary

A transverse muon polarization in $K^+ \to \pi^0 \mu^+ \nu_\mu$ would be a clear sign of T violation and is a sensitive probe for new physics beyond the Standard Model. The three Higgs-doublet model, the leptoquark model, and some supersymmetric models can give a sizable effect without conflicting with other experimental constraints. The KEK E246 experiment, using a stopped kaon beam, is aiming for an eventual statistical sensitivity of ΔP_T at the 0.1% level. All elements of the detector system are working well and the level of systematic errors has been shown to be small. The current statistical accuracy of the analyzed data is $\Delta P_T = 6 \times 10^{-3}$, or $\Delta Im\xi = 0.018$. Our results are consistent with null transverse polarization at the present time. Our experiment is scheduled to run further for 1600 hours to improve the statistics.

References

[1] KEK-PS E246 Collaboration: M. Abe,[a] M. Aoki,[b] I. Arai,[c] Y. Asano,[a] T. Baker,[d] M. Blecher,[e] M. D. Chapman,[b] D. Dementyev,[f] P. Depommier,[g] M. Grigorjev,[f] P. Gumplinger,[h] M. Hasinoff,[i] R. Henderson,[h] K. Horie,[c] W. S. Hou,[j] H. C. Huang,[j] Y. Igarashi,[c] T. Ikeda,[c] A. Ivashkin,[f] J. Imazato,[b] J-M. Lee,[k] L. S. Lee,[l] G. Y. Lim,[l] J. H. Khang,[k] W. Keil,[h] M. Khabibullin,[f] A. Khotjantsev,[f] Y. Kudenko,[f] Y. Kuno,[b] J. A. Macdonald,[h] D. R. Marlow,[m] C. R. Mindas,[m] O. Mineev,[f] C. Rangacharyulu,[d] S. K. Sahu,[j] S. Sekikawa,[c] H. M. Shimizu,[b] S. Shimizu,[n] K. Shibata,[c] Y.-M. Shin,[d] Y. H. Shin,[k] K. S. Sim,[l] A. Suzuki,[c] T. Tashiro,[c] A. Watanabe,[c] D. H. Wright,[h] T. Yokoi[o]

Address: (a) Institute of Applied Physics, University of Tsukuba, Ibaraki 305-0006, Japan.
(b) IPNS, High-Energy Accelerator Research Organization (KEK), Ibaraki 305-0801, Japan.
(c) Institute of Physics, University of Tsukuba, Ibaraki 305-0006, Japan.
(d) Department of Physics, University of Saskatchewan, Saskatoon, Canada S7N 0W0.
(e) Department of Physics, Virginia Polytechnic Institute and State University, VA 24061-0435, USA.
(f) Institute for Nuclear Research, Russian Academy of Sciences, Moscow 117312, Russia.
(g) Laboratoire de Physique Nucleaire, University de Montreal, Montreal, Canada H3C 3J7.
(h) TRIUMF, Vancouver, British Columbia, Canada V6T 2A3.
(i) Department of Physics and Astronomy, University of British Columbia, Vancouver, Canada V6T 1Z1.
(j) Department of Physics, National Taiwan University, Taipei, Taiwan.
(k) Department of Physics, Yonsei University, Seoul 120-749, Korea.
(l) Department of Physics, Korea University, Seoul 136-701, Korea.
(m) Department of Physics, Princeton University, NJ 08544, USA.
(n) Department of Applied Physics, Tokyo Institute for Technology, Tokyo 152, Japan.
(o) Department of Physics, University of Tokyo, Tokyo 113, Japan.

[2] J. J. Sakurai, Phys. Rev. **109**, 980 (1958).

[3] A. R. Zhitnitskii, Yad. Fiz. Sov. J. Nucl. Phys. **31**, 1024 (1980); *ibid* **31**, 529 (1980).

[4] R. Garisto and G. Kane, Phys. Rev. D **44**, 2038 (1991).

[5] G. Bélanger and C. Q. Geng, Phys. Rev. D **44**, 2789 (1991).

[6] M. Fabbrichesi and F. Vassani, Phys. Rev. D **55**, 5334 (1997).

[7] G. H. Wu and J. N. Ng, Phys. Lett. B **392**, 93 (1997).

[8] S. Weinberg, Phys. Rev. Lett. **37**, 657 (1976).

[9] H. Y. Cheng, Phys. Rev. D **42**, 2329 (1990).

[10] Y. Grossman, Nucl. Phys. B **426**, 355 (1994).

[11] S. R. Blatt *et al.*, Phys. Rev. D **27**, 1056 (1983).

[12] W. M. Morse *et al.*, Phys. Rev. D **21**, 1750 (1980).

[13] D. V. Dementyev *et al.*, Nucl. Instrum. Methods A **379**, 499 (1996).

[14] A. P. Ivashkin *et al.*, Nucl. Instrum. Methods A **394**, 321 (1997).

[15] Y. Kudenko and J. Imazato, KEK-Report 92-15 (1992).

[16] R. L. Wixted *et al.*, Nucl. Instrum. Methods **386**, 483 (1997).

[17] Yu. G. Kudenko, O. V. Mineev, and J. Imazato, Nucl. Instrum. Methods A **411**, 437 (1998).

[18] T. Ikeda *et al.*, Nucl. Instrum. Methods A **401**, 243 (1997).

[19] T. Yokoi, Ph.D. thesis, University of Tokyo, 1998 (unpublished).

[20] C. Mindas, Ph.D. thesis, Princeton University, 1998 (unpublished).

[21] A. Ivashkin, Ph.D. thesis, Institute for Nuclear Research, Russian Academy of Sciences, 1998 (unpublished).